

Gamma-ray sky points to radial gradients in cosmic-ray transportDaniele Gaggero,^{1,2,*} Alfredo Urbano,^{1,†} Mauro Valli,^{1,2,‡} and Piero Ullio^{1,2,§}¹SISSA, via Bonomea 265, I-34136 Trieste, Italy²INFN, sezione di Trieste, via Valerio 2, I-34127 Trieste, Italy

(Received 9 December 2014; revised manuscript received 9 February 2015; published 28 April 2015)

The standard approach to cosmic-ray (CR) propagation in the Galaxy is based on the assumption that local transport properties can be extrapolated to the whole CR confining volume. Such models tend to underestimate the γ -ray flux above a few GeV measured by the Fermi Large Area Telescope toward the inner Galactic plane. We consider here for the first time a phenomenological scenario allowing for both the rigidity scaling of the diffusion coefficient and the convective effects to be position dependent. We show that within this approach we can reproduce the observed γ -ray spectra at both low and mid Galactic latitudes—including the Galactic center—without spoiling any local CR observable.

DOI: 10.1103/PhysRevD.91.083012

PACS numbers: 98.70.Sa, 98.70.Rz

I. INTRODUCTION

Since 2008 the Fermi Large Area Telescope (Fermi-LAT) has been surveying the γ -ray sky between about a few hundred MeV and a few hundred GeV with unprecedented sensitivity and resolution. The bulk of the photons detected by the Fermi-LAT is believed to be associated with diffuse emission from the Milky Way, originated by Galactic cosmic rays (CRs) interacting with the gas and the interstellar radiation field (ISRF) via production and decay of π^0 s, inverse Compton (IC), and bremsstrahlung.

There is a striking consistency between general features in the diffuse γ -ray maps and the diffuse γ -ray flux models: the predictions mainly rely, on the side concerning emitting targets, on (indirectly) measured gas column densities and ISRF models, while, on the side of incident particles, on propagation models tuned to reproduce locally measured fluxes. When addressing at a quantitative level the quality of such a match between predictions and data, most analyses have mainly developed optimized models looping over uncertainties on the emitting targets. In particular, in Ref. [1] the authors—besides allowing for a radially dependent rescaling of the ISRF and different values of the spin temperature of the 21 cm transition—adopt a tuning of the poorly known conversion factor between the observed CO emissivities and the molecular hydrogen column densities, usually dubbed X_{CO} . In Ref. [1] it is shown that such an approach is sufficient to generate models in agreement with the data within about 15% in most regions of the sky; a remarkable exception is the fact that this procedure tends to systematically underestimate the measured flux above a few GeV in the Galactic plane region, most notably toward the inner Galaxy.

Figure 1 shows the spectrum for the γ -ray flux measured by the Fermi-LAT in the energy range between 300 MeV and 100 GeV and a large angular window encompassing the inner Galactic plane (5 years of data, within the event class ULTRACLEAN according to Fermi tools v9R32P5, as described in [2]). The yellow band corresponds to the point sources (PS) modeled using the 2-year Fermi-LAT Point Source Catalogue via a dedicated Monte Carlo (MC) code. The brown line is the contribution of the extragalactic

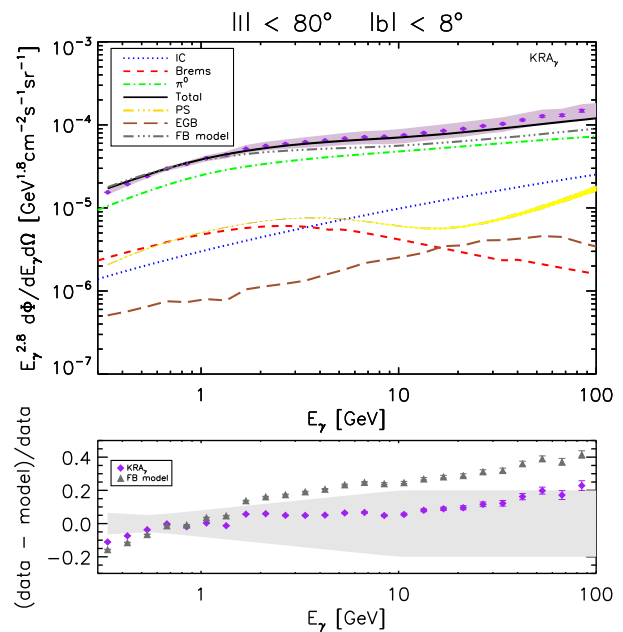


FIG. 1 (color online). Upper panel: Comparison between the γ -ray flux computed with the CR propagation model proposed in this article (a modified Kraichnan model labeled KRA_γ total flux: solid black line; individual components shown) and the Fermi-LAT data (purple dots, including both statistic and systematic errors) in the Galactic disk. For comparison, we also show the total flux for the FB model defined in Ref. [1] (double-dot-dashed gray line). Lower panel: Residuals computed for the KRA_γ and FB models.

* daniele.gaggero@sissa.it

† alfredo.urbano@sissa.it

‡ mauro.valli@sissa.it

§ piero.ullio@sissa.it

background (EGB) obtained by a full-sky fit of the data for $|b| > 20^\circ$. The double dot-dashed line and gray triangles are, respectively, the prediction and residuals for the Fermi benchmark model, labeled $^{\text{S}}\text{S}^{\text{Z}}4^{\text{R}}20^{\text{T}}150^{\text{C}}5$ (FB hereafter), selected for Fig. 17 in Ref. [1], and reproduced here using the GALPROP WebRun [3,4]: while the model is optimized at low energy, it gives a poorer description of the data at high energy, a feature that is generic for all models proposed in that analysis.

The selected angular window is interesting because the diffuse emission from the inner Galactic plane is potentially a precious source of information for CR transport modeling. Being the region with the largest gas column densities, it is the brightest zone of the sky and, unlike other regions where the interplay among components allows more modeling freedom, its flux is predominantly shaped by only one contribution, namely the π^0 decays, especially when looking at intermediate energies. The π^0 emissivity spectral index is roughly equal to the incident proton one; hence the inner Galactic plane allows an indirect measurement of the CR proton slope toward the center of the Galaxy, far away from the region where direct measurements are available. This aspect is seldom emphasized, since the standard approach consists in solving the propagation equation for CR species [5] under the assumption that diffusive properties of CRs are the same in the whole propagation volume. This implies reducing the spatial diffusion tensor to a single constant diffusion coefficient $D(\rho) = D_0(\rho/\rho_0)^\delta$, whose scaling δ on rigidity ρ and normalization D_0 are constrained by local CR data (a range between about $\delta = 0.3$ and about $\delta = 0.85$ is allowed [6–8]). Such a hypothesis freezes the proton spectral index—and therefore the π^0 spectral index—to be very close to the local one everywhere in the CR propagation region. For this reason, in Fig. 1 and in the following, the γ -ray flux is multiplied by $E_\gamma^{2.8}$, since $\gamma_p = 2.820 \pm 0.003(\text{stat}) \pm 0.005(\text{syst})$ is the proton index measured by the PAMELA experiment in the range 30 GV–1.2 TV [9]. The FB model gives a slightly rising curve since it assumes $\gamma_p = 2.72$.

The present analysis goes beyond standard approaches by allowing for spatial gradients in diffusion, using as a guideline the Fermi-LAT γ -ray data.

In the CR transport equation, the diffusion term describes at macroscopic level the effective interplay

between CRs and the magnetohydrodynamics turbulence; see, e.g., Ref. [10]. In the framework of quasilinear theory (QLT), δ is related to the turbulence spectrum (e.g., $\delta = 1/3$ for Kolmogorov-like turbulence and $\delta = 1/2$ for a Kraichnan-like one); QLT, however, assumes that the turbulent component of the magnetic field is subdominant compared to the regular one, a hypothesis that does not seem to be supported by recent models [11,12]. Studies based on nonlinear theory approaches, on the other hand, find more involved environmental dependencies, resulting in different scalings in different regions of the Galaxy, and deviations from a single power law in rigidity [13,14]. An additional element to take into account is the possibility that CRs themselves generate the turbulent spectrum responsible for their propagation [15], introducing local self-adjustments in propagation.

Given these arguments, in the following we will consider models with variable δ and show how they naturally improve the description of γ -ray data.

II. ANALYSIS

We decide to follow a data-driven approach. To quantify the change of the γ -ray slope along the Galactic disk and the resulting discrepancy between the FB model and the actual data, we show in Table I the power-law index obtained by fitting the Fermi-LAT γ -ray data in the energy window $E_\gamma = [5\text{--}50]$ GeV, and in the second row of Table II the χ^2 of the FB model.

The observed power-law index ranges from $E_\gamma^{-2.47}$ to $E_\gamma^{-2.60}$, thus resulting in a γ -ray flux much harder than the prediction of the FB model, especially in the central windows. These data should be taken as a guideline, and only show a hint of a slope change with l , instead of statistically robust evidence. We remark that, in the outermost windows we considered, the gamma-ray emission is not dominated by π^0 emission only, since the relative contributions of point sources and inverse Compton are far from being negligible.

Turning our attention to the quality of the fit for the FB model, it is worse in the innermost windows (e.g., $|l| < 10^\circ$ and $20^\circ < |l| < 30^\circ$, with $|b| < 5^\circ$), and it slightly ameliorates going toward outer longitudinal values ($50^\circ < |l| < 60^\circ$, with $|b| < 5^\circ$) but remains poor considering on average the whole Galactic disk ($|l| < 80^\circ$, with $|b| < 5^\circ$).

TABLE I. Energy slope of Fermi-LAT γ -ray data on the Galactic disk. The power-law index has been obtained by fitting the data in the energy window $E_\gamma = [5\text{--}50]$ GeV. We average in latitude over the interval $|b| < 5^\circ$.

Sky window ($ b < 5^\circ$)	α ($\Phi \sim E_\gamma^{-\alpha}$)	Sky window ($ b < 5^\circ$)	α ($\Phi \sim E_\gamma^{-\alpha}$)
$0^\circ < l < 10^\circ$	2.55 ± 0.09	$40^\circ < l < 50^\circ$	2.57 ± 0.09
$10^\circ < l < 20^\circ$	2.49 ± 0.09	$50^\circ < l < 60^\circ$	2.56 ± 0.09
$20^\circ < l < 30^\circ$	2.47 ± 0.08	$60^\circ < l < 70^\circ$	2.60 ± 0.09
$30^\circ < l < 40^\circ$	2.57 ± 0.08	$70^\circ < l < 80^\circ$	2.52 ± 0.09

TABLE II. Results of the χ^2 analysis for the fit of the Fermi-LAT γ -ray data.

χ^2 values (25 data points)	$0^\circ < l < 80^\circ$ $0^\circ < b < 8^\circ$	$0^\circ < l < 10^\circ$ $0^\circ < b < 5^\circ$	$20^\circ < l < 30^\circ$ $0^\circ < b < 5^\circ$	$50^\circ < l < 60^\circ$ $0^\circ < b < 5^\circ$	$0^\circ < l < 180^\circ$ $10^\circ < b < 20^\circ$
χ^2 KRA $_\gamma$	11.30	3.79	12.27	11.50	6.94
χ^2 FB model	53.00	74.83	70.04	24.85	17.60

To have a deeper understanding of the discrepancy, it is important to trace, for each line of sight (l.o.s.), which portion of the Galaxy the emission comes from. For this reason, in Fig. 2 we plot the relative contribution to the total π^0 emission for three reference l.o.s. as a function of the galactocentric distance, R . At large values of the Galactic longitude l (where the FB model gives a better fit) the emission is dominated by the local environment; instead, the closer to the center we look, the wider the relevant region gets, with the central rings contributing as much as 20% for the Galactic center window (where the fit is worse and the data turn out to be significantly harder). In the lower panel of Fig. 2, we show the power-law spectral index of the π^0 component as a function of R ; for the FB model, as expected, we find a constant value equal to the measured local proton spectral index.

Driven by these results, we argue that the FB model should be corrected in such a way to get a significantly harder propagated proton index for smaller values of R , and a value closer to the one inferred by Boron-to-Carbon ratio (B/C) and protons in the local region. We stress that, since

in the sky windows where the emission is mostly local (at high longitude or high latitude), the contribution of IC and point sources to total emission is relevant, we never observe a γ -ray slope equal to the local π^0 slope.

III. METHOD

We propose a propagation model based on the following three ingredients:

- (i) Bearing in mind the motivations outlined in the Introduction, we drop the oversimplified assumption of constant diffusion, and we consider the possibility that the slope of the diffusion coefficient δ is a function of R .
- (ii) We allow for position-dependent convective effects; the presence of a significant convective wind in the inner region of the Galaxy is motivated by the x-ray observations by the ROSAT satellite [16] and may affect cosmic-ray propagation [17].
- (iii) We allow for a larger value of X_{CO} in the outer part of the Galaxy; this hypothesis stems from the existence of a gradient in metallicity across the Milky Way [18]. The metallicity is a result of stellar and Galactic chemical evolution: it is higher toward the Galactic center and decreases going outwards; since lower metallicities imply less dust shielding [19], it is reasonable to expect larger values of X_{CO} for increasing R .

For this purpose, we exploit the numerical packages DRAGON [20,21] and GAMMASKY (a dedicated code recently used in [22–24] to simulate diffuse γ -ray maps).

As a starting point, we consider the Kraichnan diffusion model defined in Ref. [25] (labeled KRA therein).¹ As a first step, we modify δ introducing a functional dependence on R ; as the simplest and *a posteriori* sufficient guess, we consider $\delta(R) = AR + B$ with local normalization $\delta(R_\odot) = 0.5$, and—to avoid unrealistically large values—saturate it to $\delta(R > 11 \text{ kpc}) = \delta(R = 11 \text{ kpc})$. The free parameter A is fixed by fitting the γ -ray data in the energy range $E_\gamma = [5\text{--}50] \text{ GeV}$; to this purpose, we divide the Galactic disk $|b| < 5^\circ$, $|l| < 80^\circ$ into eight longitudinal windows of 10° each.

The energy spectra we obtain from this procedure correctly reproduce the measured slope in all the analyzed sky windows but overshoot the data at low energies, in

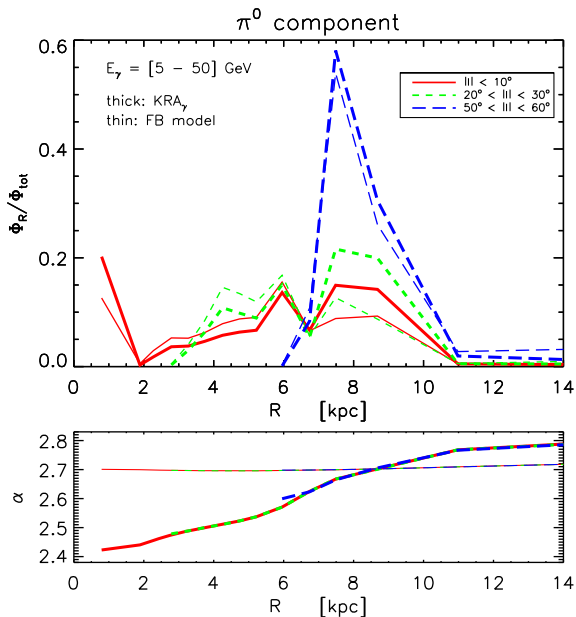


FIG. 2 (color online). Relative contribution (upper panel) and power-law spectral index of the π^0 emission (lower panel, with scaling $\sim E_\gamma^{-\alpha}$) for three reference l.o.s. as a function of the radial distance from the Galactic center. The FB (KRA $_\gamma$) model corresponds to thinner (thicker) lines. We average in latitude over the interval $|b| < 5^\circ$.

¹We checked that the same conclusions can be reached starting from the Kolmogorov and thick-halo diffusion models [25].

particular for small values of l . To tame this problem, in the inner region with $R < R_w$, we allow for a strong convective wind with a uniform gradient in the z direction. We extract R_w and the intensity of the convective gradient by fitting the low-energy data with $E_\gamma < 1$ GeV. Concerning the molecular hydrogen, we assume—in units of $10^{20} \text{ cm}^{-2} (\text{K km s}^{-1})^{-1}$ — $X_{\text{CO}} = 1.9$ at $R < 7.5$ kpc, and $X_{\text{CO}} = 5$ at $R > 7.5$, in order to correctly match the normalization of the observed flux for $|l| > 50^\circ$.

The last step of our method consists of verifying *a posteriori* that the corrections described above do not spoil the local observables: we find that just a small tuning in the value of the normalization of the diffusion coefficient D_0 and in the source spectral index γ are needed.

In particular, we checked protons (see Fig. 3), B/C (see Fig. 4), antiprotons (see Fig. 5), leptons, and $^{10}\text{Be}/^9\text{Be}$.

Concerning the beryllium ratio, the compatibility between the observational evidence of strong winds in the inner Galaxy and the constraints from the radioactive isotopes may be a problem (see, e.g., [17]). Nevertheless, in our case the Galactic wind is not present locally, and therefore we have an acceptable agreement with the data.

All in all, we report the following best-fit values for the parameters described above: $A = 0.035 \text{ kpc}^{-1}$, $R_w = 6.5 \text{ kpc}$, $dV/dz = 100 \text{ km s}^{-1} \text{ kpc}^{-1}$, $D_0 = 2.24 \times 10^{28} \text{ cm}^2 \text{ s}^{-1}$, $\gamma = 2.35$. We label this model KRA_γ .

IV. RESULTS

We show in Figs. 1, 6, and 7, the γ -ray spectra for our KRA_γ model in three relevant sky windows: the Galactic disk, a small window focused on the Galactic center, and the mid-latitude strip with $|l| < 180^\circ$, $10^\circ < |b| < 20^\circ$.

In Fig. 8 we show the longitudinal profile. We remark that the model is not optimized for high longitudes ($|l| > 100^\circ$): this is the well-known *gradient problem*, and this discrepancy can be reabsorbed by a rescaling of the π^0 component—motivated by the possible presence of neutral gas not traced by HI and CO emission lines—a position-dependent normalization of the diffusion coefficient [22], or an altered source term [36] with respect to the one we adopt [37]. A full-sky analysis based on a combined scenario with both a variable slope and normalization of the diffusion coefficient is far beyond the scope of this paper and will be addressed in a future work.

In Table II we list the χ^2 for our optimized model, showing a remarkable improvement with respect to the FB model.

There are in principle alternative scenarios leading to tilted γ -ray fluxes; see, e.g., [1,38–40]. However,

- (i) Following Ref. [41], we find that a population of unresolved pulsars, consistent with the observed counterpart, gives an extra contribution to the total γ -ray flux more than 1 order of magnitude smaller than needed.

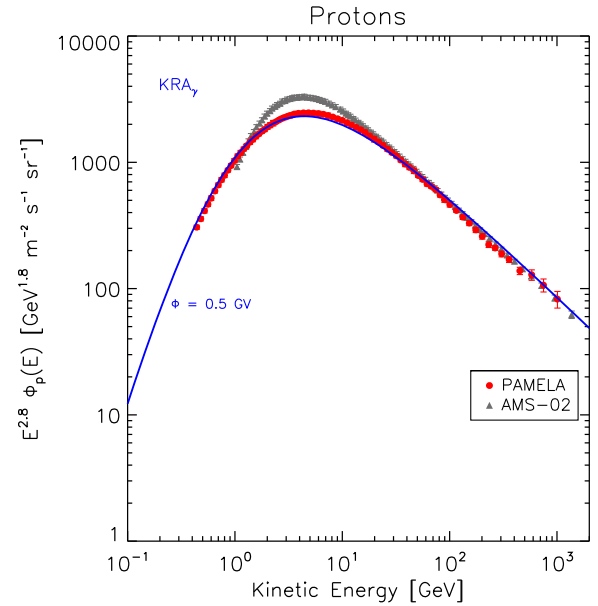


FIG. 3 (color online). Comparison between the local proton flux in the KRA_γ model and the corresponding experimental data. We use a fixed modulation potential of 500 MV, and in addition to the PAMELA data [9], we also show preliminary AMS-02 results [26].

- (ii) Running a dedicated MC code where the analytical solution of the diffusion equation with the correct boundary is implemented, as described in [42], we simulate Supernova explosions with a reasonable

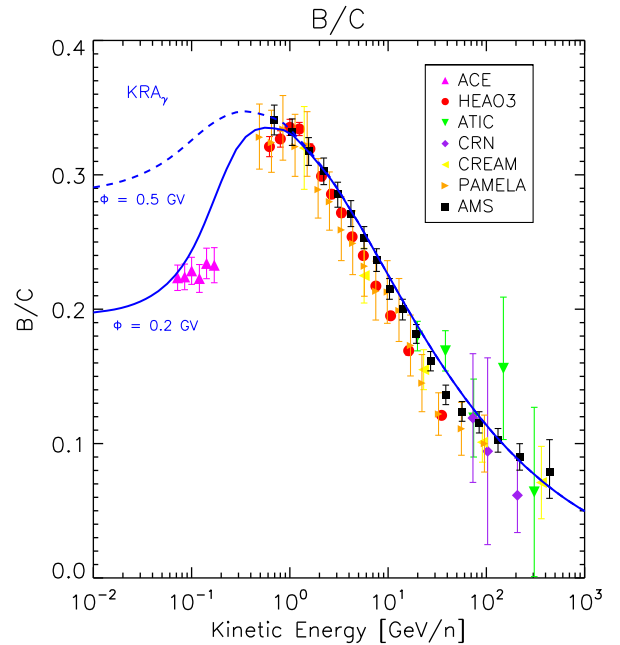


FIG. 4 (color online). Comparison between the local B/C ratio in the KRA_γ model and the corresponding experimental data. We show two different values for the modulation potential, 500 MV (dashed line) and 200 MV (solid line). Data points refer to different experiments: ACE [27], HEAO-3 [28], ATIC [29], CRN [30], CREAM [31], PAMELA [32], and AMS [33].

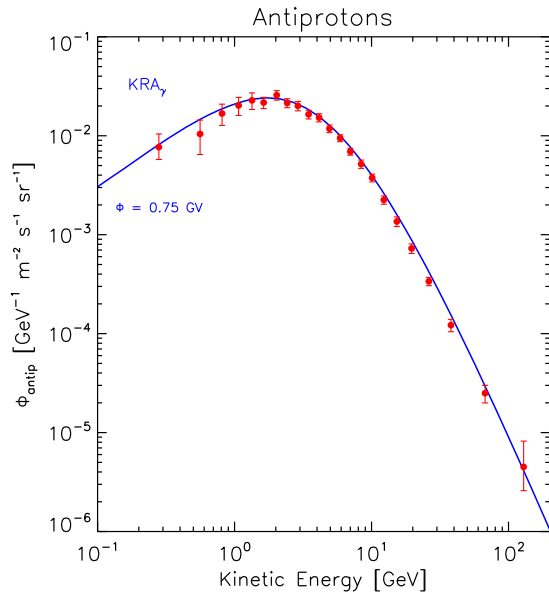


FIG. 5 (color online). Comparison between the local antiproton flux in the KRA_γ model and the corresponding PAMELA data [34]. We use a fixed modulation potential of 750 MV.

rate $\approx 3/\text{century}$ distributed according to the source term presented in [37].

We fit each realization with a power law. We find that fluctuations in the proton spectrum due to the stochasticity of the sources never exceed—even in the inner Galactic region—the few percent level.

- (iii) We test the possibility of an enhanced IC emission; we find that a rescaling of the ISRF by 1 order of magnitude, together with a factor of 10 decrease in the X_{CO} , may solve the discrepancy.

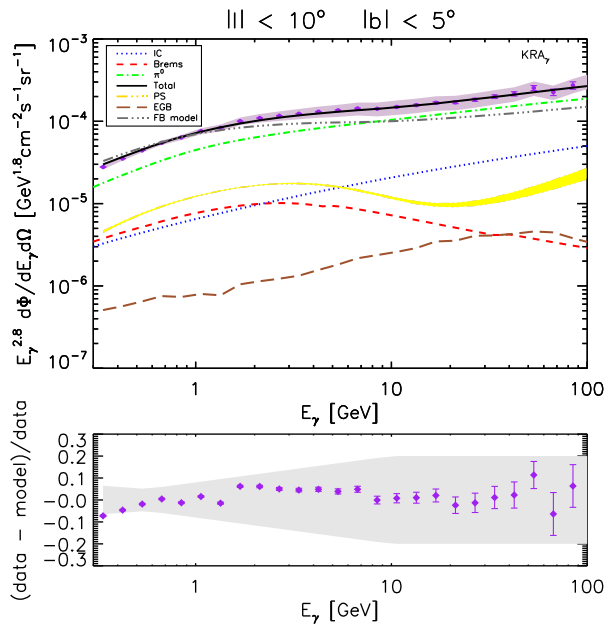


FIG. 6 (color online). The same as in Fig. 1 but considering the window $|l| < 10^\circ$, $|b| < 5^\circ$.

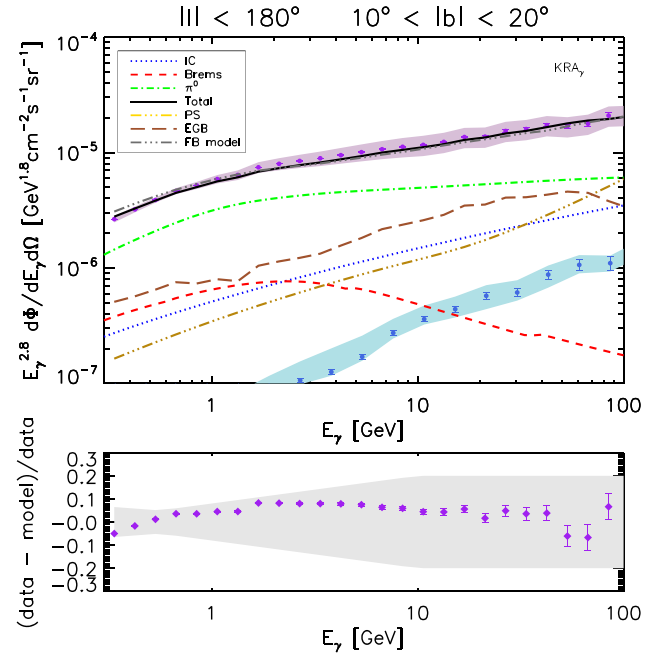


FIG. 7 (color online). The same as in Fig. 1 but considering the strip $|l| < 180^\circ$, $10^\circ < |b| < 20^\circ$. The azure band represents the contribution of the Fermi bubbles according to Ref. [35].

However, we discard this hypothesis since in this case the bulk of the γ -ray flux would have a leptonic origin, in contrast with the observed correlation with the gas distribution as shown in Fig. 8.

While the paper was undergoing the review process, the 4-year Point Source Catalog (3FGL) was released by the Fermi-LAT Collaboration. We checked that our results are not affected by this update, given the subdominant role of

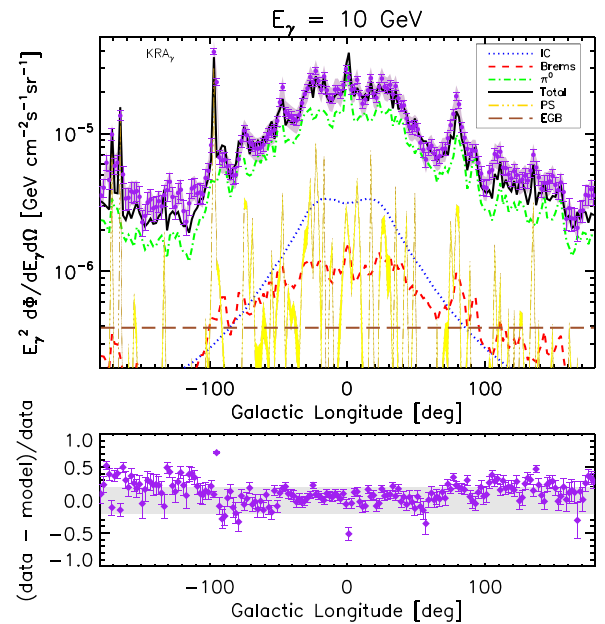


FIG. 8 (color online). Longitudinal profile at fixed energy $E_\gamma = 10$ GeV. We average in latitude over the interval $|b| < 5^\circ$.

point sources with respect to π^0 emission, especially in the windows near the Galactic center.

V. CONCLUSIONS

We addressed the problem of modeling the γ -ray emissivity in the Galaxy from a new perspective. The aim was learning how the properties of CR diffusion change through the Galaxy. Our strategy consisted of developing a CR propagation model relaxing the assumption of homogeneous diffusion: we allowed δ to vary with the galactocentric radius R . The main motivation is the discrepancy between the observed and predicted γ -ray slope: in particular, the models discussed in [1] underestimate the high-energy data in the Galactic plane region. Being the π^0 emission dominant at low latitudes, the γ -ray spectral index is determined by the proton spectrum; since the latter is well constrained by recent data, we assumed this tension to be a hint of a different diffusion regime taking place in the inner region of the Galaxy. We adopted a minimal set of assumptions (linear variation of δ , high convective regime for small R), and we found that our model reproduces the γ -ray data in many relevant windows of the sky within the systematic uncertainty. We achieved this result without relying on *ad hoc* tunings of astrophysical ingredients such as the gas distribution, the X_{CO}

conversion factor, the source distribution or the interstellar radiation field, and keeping a good agreement with locally measured CR spectra. Remarkably, in the Galactic center window our residuals do not exceed the 10% level (see Fig. 6), which is comparable with the alleged dark matter signal reported in [43–45]. A more detailed analysis with focus on this region will be presented in a forthcoming work.

ACKNOWLEDGMENTS

We thank I. Cholis, I. Gebauer, and D. Grasso for useful discussions and suggestions. The work of A. U. is supported by the ERC Advanced Grant No. 267985, “Electroweak Symmetry Breaking, Flavour and Dark Matter: One Solution for Three Mysteries” (DaMeSyFla). P. U. and M. V. acknowledge partial support from the European Union FP7 ITN INVISIBLES (Marie Curie Actions, PITN-GA-2011-289442), and partial support by the research Grant “Theoretical Astroparticle Physics” No. 2012CPPYP7 under the program PRIN 2012 funded by the Ministero dell’Istruzione, Università e della Ricerca (MIUR). In this work the authors have used the publicly available Fermi-LAT data and Fermi Tools archived at <http://fermi.gsfc.nasa.gov/ssc/>.

-
- [1] M. Ackermann *et al.*, *Astrophys. J.* **750**, 3 (2012).
 - [2] W.-C. Huang, A. Urbano, and W. Xue, arXiv:1307.6862.
 - [3] “GALPROP WebRun,” <http://galprop.stanford.edu/webrun.php>.
 - [4] A. E. Vladimirov, S. W. Digel, G. Jóhannesson, P. F. Michelson, I. V. Moskalenko, P. L. Nolan, E. Orlando, T. A. Porter, and A. W. Strong, *Comput. Phys. Commun.* **182**, 1156 (2011).
 - [5] V. S. Berezhinskii, S. V. Bulanov, V. A. Dogiel, and V. S. Ptuskin, *Astrophysics of Cosmic Rays* (North-Holland, Amsterdam, 1990).
 - [6] D. Maurin, F. Donato, R. Taillet, and P. Salati, *Astrophys. J.* **555**, 585 (2001).
 - [7] G. Di Bernardo, C. Evoli, D. Gaggero, D. Grasso, and L. Maccione, *Astropart. Phys.* **34**, 274 (2010).
 - [8] R. Trotta, G. Jóhannesson, I. V. Moskalenko, T. A. Porter, R. Ruiz de Austri, and A. W. Strong, *Astrophys. J.* **729**, 106 (2011).
 - [9] O. Adriani *et al.* (PAMELA Collaboration), *Science* **332**, 69 (2011).
 - [10] R. Schlickeiser, *Cosmic Ray Astrophysics* (Springer, New York, 2002).
 - [11] T. R. Jaffe, A. J. Banday, J. P. Leahy, S. Leach, and A. W. Strong, *Mon. Not. R. Astron. Soc.* **416**, 1152 (2011).
 - [12] R. Jansson and G. R. Farrar, *Astrophys. J.* **757**, 14 (2012).
 - [13] H. Yan and A. Lazarian, *Astrophys. J.* **673**, 942 (2008).
 - [14] C. Evoli and H. Yan, *Astrophys. J.* **782**, 36 (2014).
 - [15] P. Blasi, E. Amato, and P. D. Serpico, *Phys. Rev. Lett.* **109**, 061101 (2012).
 - [16] S. L. Snowden, R. Egger, M. J. Freyberg, D. McCammon, P. P. Plucinsky, W. T. Sanders, J. H. M. M. Schmitt, J. Trümper, and W. Voges, *Astrophys. J.* **485**, 125 (1997).
 - [17] I. Gebauer and W. de Boer, arXiv:0910.2027.
 - [18] J. Y. Cheng, C. M. Rockosi, H. L. Morrison, R. A. Schönrich, Y. S. Lee, T. C. Beers, D. Bizyaev, K. Pan, and D. P. Schneider, *Astrophys. J.* **746**, 149 (2012).
 - [19] F. P. Israel, *Astron. Astrophys.* **328**, 471 (1997).
 - [20] “DRAGON code,” <http://dragon.hepforge.org/>.
 - [21] C. Evoli, D. Gaggero, D. Grasso, and L. Maccione, *J. Cosmol. Astropart. Phys.* **10** (2008) 018.
 - [22] C. Evoli, D. Gaggero, D. Grasso, and L. Maccione, *Phys. Rev. Lett.* **108**, 211102 (2012).
 - [23] M. Tavakoli, I. Cholis, C. Evoli, and P. Ullio, arXiv:1110.5922.
 - [24] M. Cirelli, D. Gaggero, G. Giesen, M. Taoso, and A. Urbano, *J. Cosmol. Astropart. Phys.* **12** (2014) 045.
 - [25] C. Evoli, I. Cholis, D. Grasso, L. Maccione, and P. Ullio, *Phys. Rev. D* **85**, 123511 (2012).
 - [26] C. Consolandi on behalf of the AMS-02 Collaboration, arXiv:1402.0467.
 - [27] N. E. Yanasak, M. E. Wiedenbeck, R. A. Mewaldt, A. J. Davis, A. C. Cummings, J. S. George, R. A. Leske, E. C.

- Stone, E. R. Christian, T. T. von Rosenvinge, W. R. Binns, P. L. Hink, and M. H. Israel, *Astrophys. J.* **563**, 768 (2001).
- [28] J. J. Engelmann, P. Ferrando, A. Soutoul, P. Goret, and E. Juliusson, *Astron. Astrophys.* **233**, 96 (1990).
- [29] A. D. Panov *et al.*, in *Proc. 30th Int. Cosmic Ray Conf.* (Universidad Nacional Autonoma de Mexico, Mexico, 2008), Vol. 2, p. 3.
- [30] D. Mueller, S. P. Swordy, P. Meyer, J. L'Heureux, and J. M. Grunsfeld, *Astrophys. J.* **374**, 356 (1991).
- [31] H. Ahn *et al.*, *Astropart. Phys.* **30**, 133 (2008).
- [32] O. Adriani *et al.*, *Astrophys. J.* **791**, 93 (2014).
- [33] "Preliminary B/C data," <http://laspace.lsu.edu/ISCRA/ISCRA2014/Presentations/rclavero.pdf>.
- [34] A. G. Mayorov *et al.*, *J. Phys. Conf. Ser.* **409**, 012056 (2013).
- [35] M. Ackermann *et al.* (Fermi-LAT Collaboration), *Astrophys. J.* **793**, 64 (2014).
- [36] M. Ackermann *et al.* (Fermi-LAT Collaboration), *Astrophys. J.* **772**, 154 (2013).
- [37] K. M. Ferrière, *Rev. Mod. Phys.* **73**, 1031 (2001).
- [38] E. G. Berezhko and H. J. Völk, *Astrophys. J.* **611**, 12 (2004).
- [39] A. D. Erlykin and A. W. Wolfendale, *Astropart. Phys.* **42**, 70 (2013).
- [40] W. de Boer and M. Weber, *Astrophys. J. Lett.* **794**, L17 (2014).
- [41] F. Calore, M. Di Mauro, and F. Donato, *Astrophys. J.* **796**, 14 (2014).
- [42] P. Blasi and E. Amato, *J. Cosmol. Astropart. Phys.* 01 (2012) 010.
- [43] V. Vitale *et al.* (Fermi-LAT collaboration), arXiv:0912.3828.
- [44] L. Goodenough and D. Hooper, arXiv:0910.2998.
- [45] T. Daylan, D. P. Finkbeiner, D. Hooper, T. Linden, S. K. N. Portillo, N. L. Rodd, and T. R. Slatyer, arXiv:1402.6703.